

2. Virk RK, Khan A. Pseudoangiomatous stromal hyperplasia: an overview. *Arch Pathol Lab Med.* 2010;134:1070–4.
3. Raj SD, Sahani VG, Adrada BE, et al. Pseudoangiomatous stromal hyperplasia of the breast: multimodality review with pathologic correlation. *Curr Probl Diagn Radiol.* 2017;46:130–5.
4. Guatelli CS, Bitencourt AGV, Osório CABT, et al. Can diffusion-weighted imaging add information in the evaluation of breast lesions considered suspicious on magnetic resonance imaging? *Radiol Bras.* 2017;50:291–8.
5. Santucci D, Lee SS, Hartman H, et al. Comparison of Cartesian and radial acquisition on short-tau inversion recovery (STIR) sequences in breast MRI. *Radiol Bras.* 2017;50:216–23.
6. Almeida JRM, Gomes AB, Barros TP, et al. Diffusion-weighted imaging of suspicious (BI-RADS 4) breast lesions: stratification based on histopathology. *Radiol Bras.* 2017;50:154–61.
7. França LKL, Bitencourt AGV, Paiva HLS, et al. Role of magnetic resonance imaging in the planning of breast cancer treatment strategies: comparison with conventional imaging techniques. *Radiol Bras.* 2017;50:76–81.
8. Vo QD, Koch G, Girard JM, et al. A case report: pseudoangiomatous stromal hyperplasia tumor presenting as a palpable mass. *Front Surg.* 2016;2:73.
9. Celliers L, Wong DD, Bourke A. Pseudoangiomatous stromal hyperplasia: a study of the mammographic and sonographic features. *Clin Radiol.* 2010;65:145–9.
10. Jaunoo SS, Thrush S, Dunn P. Pseudoangiomatous stromal hyperplasia (PASH): a brief review. *Int J Surg.* 2011;9:20–2.
11. Kareem Z, Iyer S, Singh M. Pseudoangiomatous stromal hyperplasia: a rare cause of breast lump in a premenopausal female. *J Clin Diagn Res.* 2017;11:PD02–PD03.
12. Lee JW, Jung GS, Kim JB, et al. Pseudoangiomatous stromal hyperplasia presenting as rapidly growing bilateral breast enlargement refractory to surgical excision. *Arch Plast Surg.* 2016;43:218–21.

Tatiane Cíntia Nascimento^{1,a}, Maria Célia Djahjah^{1,b}, Ana Helena P. C. Carneiro^{1,c}, Afrânio Coelho de Oliveira^{1,d}, Edson Marchiori^{1,e}
 1. Universidade Federal do Rio de Janeiro (UFRJ), Rio de Janeiro, RJ, Brazil.
 Correspondence: Dr. Edson Marchiori. Rua Thomaz Cameron, 438, Valparaíso, Petrópolis, RJ, Brazil, 25685-120. Email: edmarchiori@gmail.com.
 a. <https://orcid.org/0000-0002-0151-2193>; b. <https://orcid.org/0000-0002-8798-9856>; c. <https://orcid.org/0000-0001-9823-0071>; d. <https://orcid.org/0000-0002-7986-8712>; e. 0000-0001-8797-7380.
 Received 10 August 2017. Accepted after revision 22 September 2017.
<http://dx.doi.org/10.1590/0100-3984.2017.0135>



Non-Hodgkin lymphoma mimicking cholangiocarcinoma

Dear Editor,

A 74-year-old white female presented with diffuse abdominal pain, jaundice, choloria, and acholia. Laboratory tests showed elevated levels of canalicular membrane enzymes. The results of a complete blood count were normal, as were serum alpha-fetoprotein levels, and a serological test for hepatitis was negative. Magnetic resonance imaging (MRI) showed a lesion in

the hepatic hilum (Figure 1A), promoting common bile duct obstruction (Figure 1B) and retroperitoneal lymph node enlargement. A lymph node biopsy was negative for malignancy, and a liver biopsy showed a diffuse large B-cell lymphoma infiltrating the liver parenchyma (Figure 1C), together with positivity for markers of Epstein-Barr virus. A positron emission tomography/computed tomography (PET/CT) study, conducted for staging, showed fluorodeoxyglucose uptake in the retroperitoneum. The patient was started on combined chemotherapy with rituximab,

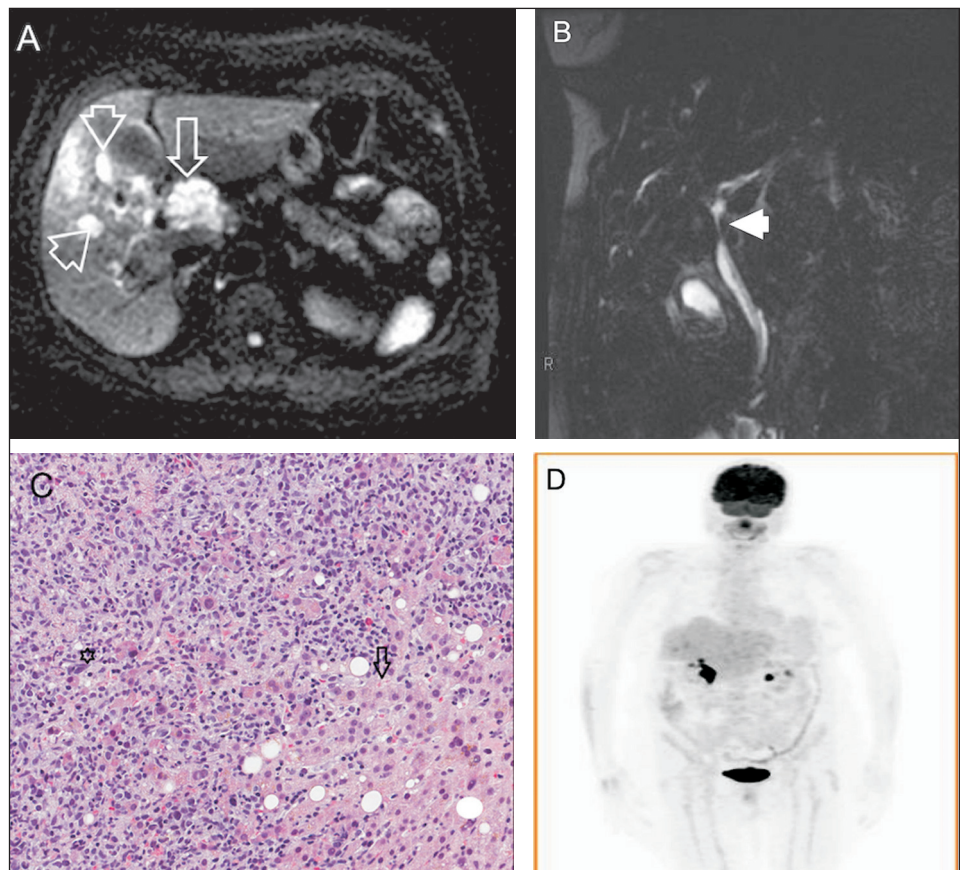


Figure 1. **A:** Axial diffusion-weighted MRI (b: 600 s/m²) showing a 4-cm expansive lesion in hepatic hilum (arrow) and small tumors focus around (arrowheads) characterized by signs of diffusion restriction, a common feature but not specific for lymphoma. **B:** Coronal strongly T2-weighted cholangioresonance showing stenosis of the common hepatic (arrowhead), related to extrinsic compression. This pattern is very similar to cholangiocarcinoma, therefore, being the main differential diagnosis. **C:** Hematoxylin-eosin staining (20x) showing lymphoid neoplasm (asterisk) characterized as diffuse large B-cell lymphoma (CD20 positive) infiltrating extensively hepatic parenchyma (arrow). **D:** Coronal fluorodeoxyglucose PET/CT showing no uptake in hepatic hilum and retroperitoneum six months after combined chemotherapy.

cyclophosphamide, adriamycin, vincristine, and prednisone. Another PET/CT study, conducted six months later, showed no evidence of disease (Figure 1D).

Hepatic lymphomas are classified as primary or secondary⁽¹⁾. Secondary lymphomas are due to disseminated lymphoproliferative disease, and the reported incidence of secondary non-Hodgkin lymphoma is 16–22%. Primary lymphomas are rare, accounting for only 0.01% of all cases of non-Hodgkin lymphoma^(1,2).

The diagnostic criteria for primary hepatic lymphoma vary in the literature, the most widely used criteria being those proposed by Lei et al.⁽¹⁾: absence of distal lymphadenopathy; absence of bone marrow infiltration or peripheral blood leukocytosis; and laboratory abnormalities related to liver involvement. Caccamo et al.⁽²⁾ included the absence of extrahepatic disease for at least six months after diagnosis. However, some authors have also classified patients with associated regional lymph node disease, splenomegaly, and bone marrow infiltration as having primary hepatic lymphoma, those features being considered indicative of regional extrahepatic evolution^(3–5). The etiology is poorly understood, and there have been reports of cases related to viral infections, such as HIV infection, Epstein-Barr virus infection, and hepatitis, as well as to cirrhosis, prior chemotherapy, and primary biliary cirrhosis^(1,6). The usual symptoms are those associated with involvement of the liver parenchyma, such as jaundice, abdominal pain, and hepatomegaly⁽¹⁾, similar to those of primary lymphoma described in the literature^(1,3,7) and well characterized in our patient due to a common bile duct obstruction. Fever, weight loss, and night sweats, also known as “B symptoms”, may be present but are not the rule⁽¹⁾. Elevated levels of canalicular enzymes is a common laboratory finding⁽¹⁾.

The imaging features of primary lymphomas are nonspecific and may be similar to those of other more common liver tumors, such as cholangiocarcinoma⁽⁸⁾. High-grade lymphomas usually show restricted diffusion on MRI, similar to what was observed in our patient but also seen in some infectious processes, such as abscess and fungal infections, in patients who are immunocompromised⁽⁸⁾, which our patient was not.

According to the current criteria in the literature, our patient had aspects indicative of primary and secondary hepatic lymphoma. Although the biopsy of an enlarged retroperitoneal lymph node was negative for malignancy, the PET/CT scan showed retroperitoneal fluorodeoxyglucose uptake. Although the diagnosis can be made through needle biopsy, it is often made after surgical resection. The standard treatment is systemic chemotherapy^(6,8).

REFERENCES

1. Lei KI, Chow JH, Johnson PJ. Aggressive primary hepatic lymphoma in Chinese patients. Presentation, pathologic features, and outcome. *Cancer*. 1995;76:1336–43.
2. Caccamo D, Pervez NK, Marchevsky A. Primary lymphoma of the liver in the acquired immunodeficiency syndrome. *Arch Pathol Lab Med*. 1986;110:553–5.
3. Osborne BM, Butler JJ, Guarda LA. Primary lymphoma of the liver. Ten cases and a review of the literature. *Cancer*. 1985;56:2902–10.
4. Anthony PP, Sarsfield P, Clarke T. Primary lymphoma of the liver: clinical and pathological features of 10 patients. *J Clin Pathol*. 1990;43:1007–13.
5. Scoazec JY, Degott C, Brousse N, et al. Non-Hodgkin's lymphoma presenting as a primary tumor of the liver: presentation, diagnosis and outcome in eight patients. *Hepatology*. 1991;13:870–5.
6. Ugurluer G, Miller RC, Li Y, et al. Primary hepatic lymphoma: a retrospective, multicenter rare cancer network study. *Rare Tumors*. 2016;8:6502.
7. Steller EJ, van Leeuwen MS, van Hillegersberg R, et al. Primary lymphoma of the liver – a complex diagnosis. *World J Radiol*. 2012;4:53–7.
8. Tomasian A, Sandrasegaran K, Elsayes KM, et al. Hematologic malignancies of the liver: spectrum of disease. *Radiographics*. 2015;35:71–86.

Gustavo Gomes Mendes^{1,a}, Leonardo Verza^{1,b}, Tércia Neves^{1,c}, Eduardo Nóbrega Pereira Lima^{1,d}, Rubens Chojniak^{1,e}

1. A.C.Camargo Cancer Center, São Paulo, SP, Brazil.

Correspondence: Dr. Leonardo Verza. A.C.Camargo Cancer Center – Departamento de Imagem. Rua Professor Antônio Prudente, 211, Liberdade. São Paulo, SP, Brazil, 01509-010. Email: leoverza9@gmail.com.

a. <https://orcid.org/0000-0001-5630-7966>; b. <https://orcid.org/0000-0002-1287-6056>; c. <https://orcid.org/0000-0002-9209-0300>; d. <https://orcid.org/0000-0003-1608-6964>; e. <https://orcid.org/0000-0002-8096-252X>.

Received 10 August 2017. Accepted after revision 9 October 2017.

<http://dx.doi.org/10.1590/0100-3984.2017.0134>



Mounier-Kuhn syndrome: an unusual cause of bronchiectasis

Dear Editor,

A 49-year-old nonsmoking man presented with a six-year history of recurrent infections of the lower respiratory tract, having been asymptomatic between the episodes. The initial physical examination showed that the patient was in good general health, with a blood pressure of 120/80 mmHg, normal cardiac auscultation findings, a heart rate of 77 bpm, pulmonary auscultation showing sparse rales, a respiratory rate of 18 breaths/min, oxygen saturation of 93% on room air, and a normal abdomen. A computed tomography (CT) scan of the chest, acquired during inspiration (Figures 1A, 1B, and 1C), showed dilatation of the trachea and main bronchi (transverse diameter of 3.5 cm and 1.8 cm, respectively), as well as bronchiectasis in the middle and lower regions of both lungs. A slice acquired during expiration (Figure 1D) demonstrated partial collapse of the trachea and main bronchi. The pattern seen on CT was considered to be diagnostic of tracheobronchomegaly. Spirometry produced the following results before and after bronchodilator administration, respectively: FVC, 87% and 88%; FEV₁, 69% and 75%; FEV₁/FVC ratio, 64% and 69%; and FEF, 44% and 52%. The

patient was treated with corticosteroids and bronchodilators. At this writing, he is in outpatient follow-up.

The importance of tracheobronchial diseases has been emphasized in recent studies^(1–4). Tracheobronchomegaly, or Mounier-Kuhn syndrome, is a rare disease, observed mainly in middle-aged men before the fifth decade of life⁽⁵⁾, that is characterized by atrophy or the absence of elastic fibers or smooth muscle in the wall of the trachea and the main bronchi, resulting in dilatation of those structures^(6–8). It is believed that the weakness of connective tissue, associated with the inhalation of air pollutants and smoking, is the main factor in the development of this condition⁽⁶⁾. Because of those anatomical and physiological changes, the flaccid airways widen during inspiration and collapse during expiration⁽⁶⁾; in addition to that dynamic change, bronchial or tracheal diverticulosis and bronchiectasis are common^(7,8).

The clinical presentation of Mounier-Kuhn syndrome is nonspecific, including the accumulation of secretions, with productive cough, dyspnea, and recurrent infections of the lower respiratory tract. In rare cases, there can be hemoptysis or pneumothorax^(6–8). The diagnosis is made on the basis of imaging findings. The most sensitive examination is CT of the trachea and main bronchi, with images acquired during inspiration and